which in practice has been recognized by treating a series of BB-n polyesters.[6]

Conclusion

Two distinct smectic layer structures were observed for BB-5 and BB-6 smectic mesophases. In the BB-6 mesophase, both the axes of the polymer chain and the mesogenic group lie perpendicular to the smectic layer planes. This type of smectic mesophase can be classified as smectic A. In BB-5, the mesogenic groups are tilted by about 25° to the layer normal, although the polymer chains lie parallel to it. The mesophase in this case is a new type of smectic C in which the tilt direction of mesogenic groups is invariable in each second neighboring layer but opposite to each other between the layers of nearest neighbors. Such a different formation of smectic layer structure between BB-5 and BB-6 can be appreciated by the average conformation of the polymer chain, which conforms to the orientational order of the mesophase and so appears with different features, depending on the even–odd parity of the carbon numbers in the flexible spacer.

Registry No. BB-5 (SRU), 81192-66-7; BB-5 (copolymer), 81197-18-4; BB-6 (SRU), 50602-05-6; BB-6 (copolymer), 81197-19-5.

References and Notes

(1) Watanabe, J.; Hayashi, M. *Macromolecules* **1987**, *21*, 278.
(2) Krigbaum, W. R.; Watanabe, J. *Polymer* **1983**, *24*, 1299.
(3) Leadbetter, A. J.; Norris, E. K. *Mol. Phys.* **1979**, *38*, 669.
(4) Leadbetter, A. J.; Wrighton, P. G. *J. Phys. Colloq.* **1979**, *40*, C3-224.
(5) Gray, G. W.; Goodby, J. W. G. *Smectic Liquid Crystals*; Leonard Hill: Glasgow and London, 1984.
(6) Watanabe, J.; Hayashi, M., unpublished results.
(7) de Vries, A.; Ekachai, A.; Spielberg, N. *Mol. Cryst. Liq. Cryst.* **1979**, *49*, 143.
(8) Abe, A. *Macromolecules* **1984**, *17*, 2280.
(9) Abe, A.; Furuya, H. *Kobunshi Ronbunshu* **1986**, *43*, 247.
(10) Abe, A.; Furuya, H. *Polym. Bull.* **1988**, *19*, 403.
(11) Abe, A.; Furuya, H.; Yoon, Do Y. *Mol. Cryst. Liq. Cryst.* **1988**, *159*, 151.
(12) Abe, A.; Furuya, H. *Mol. Cryst. Liq. Cryst.* **1988**, *159*, 99.
(13) de Vries, A. *J. Phys. Lett.* **1974**, *35*, L-139.
(14) De Jeu, W. H.; De Poorter, J. A. *Phys. Lett.* **1977**, *61A*, 114.
(15) Wulf, A. *Phys. Rev. A* **1978**, *17*, 2077.
(16) Watanabe, J.; Morita, A.; Hayashi, M., unpublished data.
(17) In contrast to this, the chiral smectic C induced on the normal smectic C of polyester

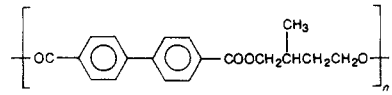

has been found to be ferroelectric.[16]
(18) Michelson, A.; Cabid, D.; Benguigui, L. *J. Phys.* **1977**, *38*, 961.

Phase Behavior of a Semiflexible Polymer with both Thermotropic and Lyotropic Properties[1]

Christopher Viney[2] and Do Y. Yoon*

IBM Almaden Research Center, 650 Harry Road, San Jose, California 95120-6099

Bernd Reck and Helmut Ringsdorf

Institut für Organische Chemie, Universität Mainz, D-6500 Mainz, FRG.

Received November 17, 1988; Revised Manuscript Received March 2, 1989

ABSTRACT: A semiflexible polymer, comprising rodlike groups connected by spacer groups in alternating succession in the main chain and also rigid side groups attached to each backbone rodlike unit via a spacer, has been found to exhibit both thermotropic and lyotropic behavior. The polymer shows isotropic–nematic biphasic separation over a wide concentration range of 20–100% by volume in the temperature range of 25–268 °C. The resulting phase diagram therefore has a strongly bent chimney shape, in contrast to the nearly vertical chimney obtained with rigid rodlike polymers. Comparison of experimental results with the predictions of Flory and Warner on rodlike molecules with orientation-dependent interactions shows that the spacer groups in the main chain do not behave like free joints. The unique phase behavior is therefore attributed to the strong influence of the degree of flexibility of the spacer groups on the cooperative alignment of neighboring rodlike moieties in the ordered state.

Introduction

Isotropic–anisotropic biphasic equilibria have been investigated extensively for a number of liquid-crystalline systems, and their phase behavior characteristics are described satisfactorily by molecular theory.[3] These examples include rodlike polymers and mixtures of rods in solution,[4] mixtures of thermotropic rodlike molecules of different lengths,[5,6] mixtures of rodlike polymers and flexible polymers,[3,7] and semiflexible polymers in solution.[3,8] Flory and his collaborators, in particular, have been quite successful in describing these diverse systems with a molecular theory that employs a lattice model and thus emphasizes the major contributions of steric repulsions, augmented by soft orientation-dependent attractions.[9]

Recently, much attention has been focused on a new class of liquid-crystalline polymers comprising rodlike and flexible groups in alternating succession in the chain backbone, due to the appearance of isotropic–anisotropic transitions of polymer melts at experimentally accessible temperatures.[10-13] There are now a large number of experimental results on the thermotropic phase behavior of these semiflexible polymers. Theoretical understanding, however, is just beginning and is limited to some empirical descriptions of thermodynamic and molecular phenomena.[14] There exists virtually no experimental work on the phase behavior and the molecular order of these semiflexible thermotropic polymers in the presence of solvents. Experiments on lyotropic systems of this class of polymers, covering a wide concentration range, should provide much deeper insights into their order–disorder phase behavior and will also provide a stringent test for any emerging theoretical work.

In this paper we present the experimental results of isotropic–nematic biphasic separation of such a semiflex-

0024-9297/89/2222-4088$01.50/0

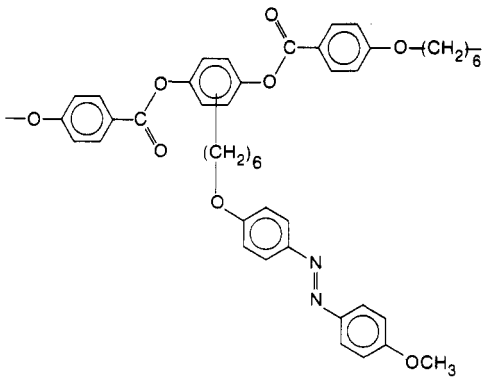

Figure 1. Schematic of the combined main- and side-chain liquid-crystalline polymer used in our experiments.

ible polymer system over a wide polymer concentration of 20–100% by volume. We then compare our experimental results with the theoretical predictions of Flory and Warner[15] calculated for rodlike molecules with orientation-dependent (thermotropic) interactions, in order to assess whether the spacer groups can be treated as free joints[16] and, if not, how strongly the degree of flexibility of the spacer groups affects the "cooperative" alignment of neighboring rigid groups in the nematic state.

Experimental Section

Polymer Sample. Our study was centered on the polymer shown schematically in Figure 1. Its synthesis is described in detail in ref 17. The polymer has an inherent viscosity $\eta_{inh} = 0.6$ dL/g at 0.5 g/dL concentration in 1,1,2,2-tetrachloroethane at 25 °C, and from GPC, the weight-average molecular weight is estimated to be ca. 38 000 in terms of polystyrene standard.[18] A previous study,[17] using optical microscopy and differential scanning calorimetry, identified a glass transition at 56 °C and a nematic-to-isotropic transition at 268 °C. In addition, the polymer appears to undergo a smectic-like to nematic transition at around 160 °C,[18] with a very small (<1 J/g) but reversible enthalpy change. However, this transition is not relevant to our study, insofar as our main interest is focused on the isotropic–nematic transition in the presence of solvents.

A tetrachloromethane/ethanol density gradient column was used to measure the room temperature (20 °C) density of the polymer. To prevent porosity from contributing to the density measurement, as-synthesized particles were first heated to 200 °C, allowed to fuse, and cooled slowly to room temperature. The measured density is 1234 ± 2 kg·m^{-3}.

Preparation of Solutions of Known Concentration. It was observed qualitatively that the polymer forms lyotropic phases in the following solvents: (1) 1,1,2,2-tetrachloroethane (TCE; boils at 146.5 °C when pure); (2) *m*-dibromobenzene (DBB; dissolves polymer at temperatures above approximately 56 °C and boils at 219 °C when pure); (3) *o*-dichlorobenzene (DCB; dissolves polymer at temperatures above approximately 39 °C and boils at 178 °C when pure).

Although initial formation of a solution required heating in the case of solvents DBB and DCB, such solutions were found to be stable on subsequent cooling to room temperature.

Solutions were prepared in glass capillaries having an internal diameter of 1 mm. While final concentrations are expressed in terms of volume percent (or volume fraction) of polymer, the concentration is most easily and accurately determined by measuring the *mass* of the separate components. Specimens of accurately known concentration were prepared according to the following procedure (modified from ref 4 and 19): A length of capillary (approximately 5 cm) was flame sealed at one end, a small quantity (~1 mg) of coarse iron filings was added, and the system was weighed. A quantity of polymer was introduced, and the system was weighed again. Next, an excess of solvent was introduced with a syringe, dissolving the polymer to give a clear orange solution; a magnet was used to agitate the iron filings and thus stir the solution. Solvent was allowed to evaporate, over a period of days if necessary, until the mass of the system equaled

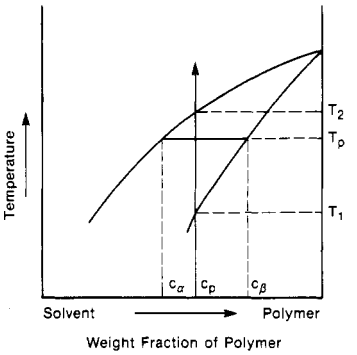

Figure 2. Schematic representation of experimentally determined polymer–solvent phase diagram, with the abscissa scale in weight fraction of polymer. The temperature T_1 is identified when isotropic regions first appear in the optical microstructure of the specimen having overall composition c_p, as the specimen is heated at 1 °C/min. Similarly, T_2 is identified when the last resolvable anisotropic regions disappear on heating. Compositions c_α and c_β are defined as the compositions at the ends of the tie line for temperature T_p.

that calculated to correspond to the desired solution concentration. This route to specimen preparation is preferred to directly mixing the components in their final proportions, since the kinetics of dissolution are slow for high polymer concentrations, and the attainment of an equilibrium solution is less certain in such cases.[20]

The concentration of a specimen could be maintained indefinitely by sealing the open end of the capillary. When necessary, the concentration could be changed subsequently by breaking off the seal, weighing the system, and allowing the appropriate mass of solvent to evaporate. Stirring and the evaporation of solvent from concentrated solutions were facilitated if the capillaries were immersed in a heated oil bath. To discourage a polymer residue from adhering to the capillary walls as the level of solution dropped during solvent evaporation, the capillary was periodically placed in a bench-top centrifuge (International Equipment Co., Boston, MA) and spun at 750*g* for up to 10 min. Any phase separation resulting from centrifuging was destroyed by subsequent stirring with the iron filings.

Specimens for hot-stage optical microscopy were produced via the above route; sealed ends of the capillary were then cut off cleanly with a diamond scribe, a length of flexibe tube was inserted over one end, and some of the contents of the capillary were deposited on a glass of microscope slide by blowing gently into the tube. The iron filings were retained in the capillary by a magnet. A glass coverslip was immediately placed over the specimen and sealed in position with Torr Seal resin (Varian Associates, Vacuum Products Division, Lexington, MA). Care has to be taken to avoid contamination of the specimen by contact with the uncured resin. Cured resin was tested for stability to long-term exposure to solvent, by immersing beads of known mass in pure solvent. The mass of the beads remained unchanged after a week, and no deposit was observed when the solvent was evaporated from a glass microscope slide.

Qualitative Characterization of Phases. Specimens were observed between crossed polars in a Zeiss (Jena) Amplival polarizing microscope. A Mettler hotstage (FP82) and controller (FP80) were used for above-ambient work. Isotropic, nematic, and biphasic (isotropic + nematic) textures were observed.

Both the color and the transparency of bulk solutions as prepared in capillaries were found to correlate with the microscopic observations of phase, as follows: isotropic, orange and clear; biphasic, orange and turbid; nematic, yellow and opaque.

Quantitative Characterization of Phases. Microscopic observation of optical texture as a function of temperature allowed measurement of the transition temperatures between nematic and biphasic and between biphasic and isotropic, for specimens of any given composition. Results can be plotted as a phase diagram with the abscissa either scaled in weight fraction of polymer (shown schematically in Figure 2) or rescaled in terms of volume fraction.

The phase diagram obtained by microscopy was checked by three other methods for consistency with equilibrium conditions.

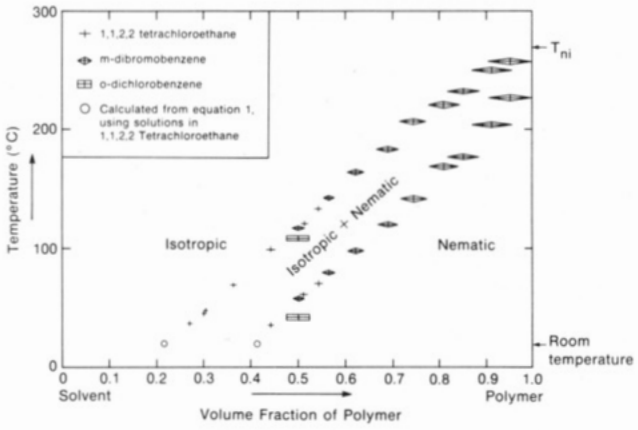

Figure 3. Experimentally determined phase diagram for the polymer in various solvents. The abscissa is scaled in terms of volume fraction of polymer. The height and width of each symbol represents the error associated with the data. All the data, except for the two cases represented by open circles, were obtained by optical microscopy. The data represented by open circles were obtained from eq 1.

First, the fractions (by area) of isotropic and nematic phase were estimated microscopically for specimens of composition c_p and temperature T_p plotted in the biphasic region of the diagram (see Figure 2). The area fractions are approximately equal to the volume fractions, since the specimens used for microscopy are thin (≤5 μm). To a first approximation, one can also assume that both phases have the same density. Thus their area fractions can be taken as a measure of their weight fractions. One can therefore use the lever rule[21] (which applies specifically under conditions of equilibrium) to predict the ratio $(c_\beta - c_p)/(c_p - c_\alpha)$ for the tie line at T_p and then compare this with the diagram already determined. When using the lever rule, it is necessary for the experimentally determined phase diagram to be scaled in terms of the weight fraction of the polymer and to assume that the polymer molecules in the two phases have an identical molecular weight distribution.

A second check, more accurate but also more laborious, involved selecting three compositions c_p, c_q, and c_r plotting on a given tie line. From the lever rule, one can show that

$$c_\alpha = \frac{c_q(1 + \rho R_q) - c_p(1 + \rho R_p)}{\rho(R_q - R_p)} \tag{1a}$$

Here R represents the microscopically observed ratio of isotropic phase area to anisotropic phase area in a specimen. The quantity ρ represents ρ_α/ρ_β, i.e., the ratio of the densities of the two phases in equilibrium is now taken into account, though its actual value is unknown. A similar equation may be written for any two of the specimens p, q, and r. One can therefore solve for the two unknowns ρ and c_α and then calculate c_β using

$$\frac{c_\beta - c_p}{c_p - c_\alpha} = \rho R_p \tag{1b}$$

The calculated values of c_α and c_β should agree with those at the end of the appropriate tie line on the phase diagram as plotted.

A third check involved using a melting point apparatus (Thomas Uni-Melt; Arthur H. Thomas Co., Philadelphia, PA) to follow the transitions as specimens of known composition were heated in the capillaries in which they were prepared. Also, the volume fractions of the isotropic and the anisotropic phase in equilibrium at room temperature could be estimated by first centrifuging the capillary at 750 g for 30 min to separate the phases into two layers and then measuring the height of the layers. Though restricted to room temperature, this method of measuring volume fractions has distinct advantages over the microscopic measurement of relative area fractions: it is simple, referring directly to three dimensions, and it concentrates the phases into resolvable volumes. When using the microscopic technique, there is always the concern that a significant fraction of a particular phase may be distributed in domains that are too small to be resolved by the objective.

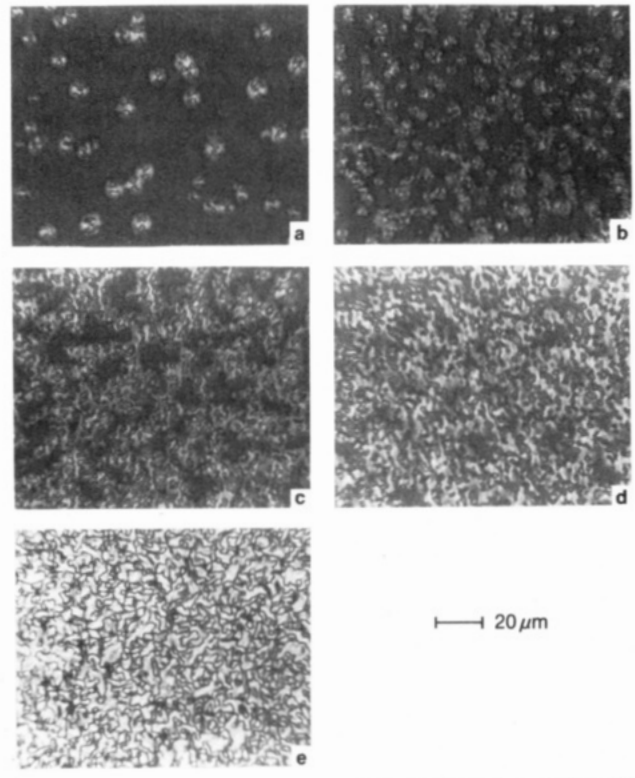

Figure 4. Optical microstructures of polymer solutions in TCE at room temperature. The volume fraction of polymer in each specimen is (a) 0.25, (b) 0.30, (c) 0.35, (d) 0.38, and (e) 0.45. Specimens a–d are biphasic (isotropic + nematic), while (e) is single-phase nematic. The micrographs as printed represent about 10% of the field of view in the microscope; the relative amounts of isotropic and nematic phase seen in (a)–(d) need therefore not be exactly representative of the entire specimen.

The Phase Diagram As Determined Experimentally

Results for the polymer in solvents TCE, DBB, and DCB are shown in Figure 3. It is immediately apparent that the first two solvents give compatible results, but not the third. The data obtained with DBB allow us to extend the range of our measurements from above the boiling point of TCE to the nematic–isotropic transition T_{ni} of the pure polymer. Though pure DBB boils at 219 °C, it was possible to make microscopic observations reproducibly at up to 260 °C in highly concentrated solutions of maximum polymer volume fraction equal to 0.95. The errors associated with measuring small changes in the mass of a small total amount of solvent become significant with high concentrations; this is also illustrated in Figure 3. When solutions of the polymer in DBB are cooled below 56 °C (the approximate temperature required for the polymer to dissolve), they behave as though the solvent were TCE, and the microstructures are stable indefinitely at room temperature.

Previous work also has demonstrated that the phase behavior of a liquid-crystalline polymer may be similar in some solvents but somewhat different in others.[4,22-24] This may reflect the contributions of the polymer–solvent interactions (χ), especially the concentration dependence of χ.

Typical microstructures of biphasic specimens at room temperature are shown in Figure 4, illustrating how the relative fraction of anisotropic phase changes with polymer concentration. The micrographs were obtained at room temperature to allow access with a high numerical aperture objective and thus achieve optimum resolution. When a single-phase nematic specimen is heated, the sequence of

textures and morphologies changes as though the system were becoming progressively more dilute at constant temperature. The schlieren texture of the anisotropic phase is characteristic of nematic ordering in a polymer, with the disclination density being higher (and the schlieren texture being finer) than in low molecular weight nematics.[25] Textures in polymer liquid crystals are more stable to realignment by external conditions, compared to the textures in small-molecule liquid crystals.[26] We therefore do not observe the "classical" schlieren texture in which molecules tend to align parallel to the glass boundary surfaces.

The Phase Diagram for Freely Jointed Rods

Our theoretical interest in determining the form of the polymer–solvent binary phase diagram was to test the applicability of the freely jointed chain (Kuhn model). In this model, the polymers can be replaced by "equivalent" short rods connected by free joints. The phase behavior for such a system should be practically identical with that of "equivalent" short rods,[16] calculated previously by Warner and Flory.[15] This method takes account both of hard-rod steric interactions and of the existence of anisotropic intermolecular forces.

Nematic–isotropic equilibrium requires that

$$(\mu_s - \mu_s^0)_{\text{nematic}} = (\mu_s - \mu_s^0)_{\text{isotropic}} \tag{2a}$$

and

$$(\mu_p - \mu_p^0)_{\text{nematic}} = (\mu_p - \mu_p^0)_{\text{isotropic}} \tag{2b}$$

The symbol μ denotes chemical potential, and the subscripts s and p refer to solvent and polymer, respectively. According to Warner and Flory, the chemical potentials in eq 2a and 2b are expressed by

$$(\mu_s - \mu_s^0)_{\text{nematic}} = RT\left[\log(1 - v_n) + a + \frac{v_n}{x}(\bar{y} - 1) + \frac{v_n^2 s^2}{2\theta}\right] \tag{3a}$$

$$(\mu_s - \mu_s^0)_{\text{isotropic}} = RT\left[\log(1 - v_i) + \frac{v_i}{x}(x - 1)\right] \tag{3b}$$

$$(\mu_p - \mu_p^0)_{\text{nematic}} = RT\left[\log\left(\frac{v_n}{x f_1}\right) + v_n(\bar{y} - 1) - \left(\frac{x v_n s}{\theta}\right)\left(1 - \frac{v_n s}{2}\right)\right] \tag{3c}$$

$$(\mu_p - \mu_p^0)_{\text{isotropic}} = RT\left[\log\frac{v_i}{x} + v_i(x - 1)\right] \tag{3d}$$

Quantities used in these equations are defined as follows: x is the axial ratio of the rods; v_i is the volume fraction of polymer in the isotropic phase; v_n is the volume fraction of polymer in the anisotropic phase

$$a = -\log\left[1 - v_n\left(\frac{\bar{y}}{x}\right)\right] \tag{4}$$

$$\bar{y} = (4/\pi)x(f_2/f_1) \tag{5}$$

s is the order parameter for the rods. It is defined as $s = 0.5\,(3 < \cos^2\psi > -1)$, where ψ is the angle between the axis of an individual rod and the preferred alignment direction. It should not be confused with the subscript s that is used to indicate the solvent.

θ is a reduced temperature T/T^*, where T is the actual temperature and T^* is a scaling temperature, representative of the intensity of the orientation-dependent intermolecular forces per chain segment of unit axial ratio.[3,5,6] In the present work T^* is chosen so that the calculated T_{ni} for the pure polymer matches the experimentally determined value of 268 °C (see below).

$$f_j = \int_0^{\pi/2} \sin^j\psi \exp\left[-x\left(\frac{4}{\pi}a + \frac{3}{2}\frac{v_n s}{\theta}\sin\psi\right)\sin\psi\right] d\psi \tag{6}$$

The derivation of eq 3a–d also gives rise to the following self-consistentcy condition:[15]

$$s = 1 - \frac{3}{2}\frac{f_3}{f_1} \tag{7}$$

For the present paper, theoretically predicted phase diagrams with composition (volume fraction of polymer) as the abscissa and temperature as the ordinate were calculated from the above equations according to the following algorithm: (1) Choose appropriate fixed values of x and T^*. (2) Guess starting values of v_i, v_n, a, and s. (3) Set T equal to the lower limit of the range to be covered by the phase diagram. (4) Apply the Newton-Raphson iteration method for equations in two variables[27] to eq 4 and 7, to refine the values for a and s. The integral in eq 6 was evaluated by Simpson's rule, sampling at intervals of half a degree. (5) Using the refined values of a and s, apply the Newton-Raphson method to eq 2a,b, to recalculate v_i and v_n. If these values need to be refined, return them to step 4 above. Repeat as necessary, to obtain the points at the end of a single tie line on the phase diagram. (6) Increment T, and repeat from step 4.

The appropriate fixed value of T^* in step 1 above is found by first calculating θ as predicted by theory for the nematic–isotropic transition in the pure polymer. For the pure polymer ($v_n = v_i = 1$), eq 2b, with substitution of eq 3c,d, gives

$$x - \bar{y} + \log f_1 + \frac{xs}{\theta}\left(1 - \frac{s}{2}\right) = 0 \tag{8}$$

An algorithm is now used to find θ: (1) Choose the fixed value of x. (2) Guess starting values of a, s, and θ. (3) Apply the Newton-Raphson iteration method to eq 4 and 7, to refine the values for a and s. (4) Using the refined values of a and s, apply the Newton-Raphson iteration method to eq 8, to recalculate θ. If this value needs further refinement, return it to step 3 above; repeat as necessary.

T^* is obtained from θ, from the experimentally measured T_{ni} of 268 °C.

Comparison of Theory and Experiment

Consideration of the bond lengths and angles in the polymer molecule suggests that an axial ratio of between 3 and 4 appropriately describes the rodlike segments. The values of T^* required to match the theoretical and experimental plots at T_{ni} of the neat polymer were 520 and 297 K for rod axial ratios of 3 and 4, respectively. These values are consistent with the estimates of T^* made by Ballauff and Flory[6] for *p*-oxybenzoate oligomers. From the phase transition and equation of state data for the trimer, tetramer, and pentamer, they obtained T^* in the range 306–343 K, taking the reduced volume $\tilde{V}$ at the transition to be 1.2–1.4. The value of T^* corresponding to our eq 8, derived for $\tilde{V} = 1$, is then ca. 250 K for the *p*-oxybenzoate moiety.

Figure 5 shows calculated phase diagrams for $x = 3$ and $x = 4$, superimposed on a plot of the experimental data. Comparison of the two theoretical plots in Figure 5 suggests that a better fit with experiment might be obtained

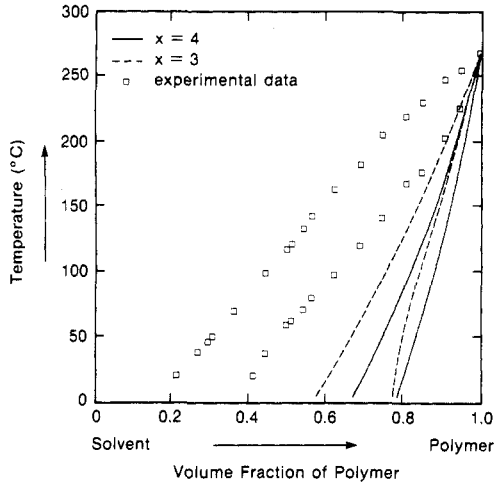

Figure 5. Calculated phase diagrams for $x = 4$ (solid lines) and $x = 3$ (broken lines). Values of $T^* = 297$ K and $T^* = 520$ K, respectively, were used to match the calculated value of T_{ni} to the experimentally measured value of 268 °C. Experimental data have been superimposed on the calculated diagrams as individual symbols.

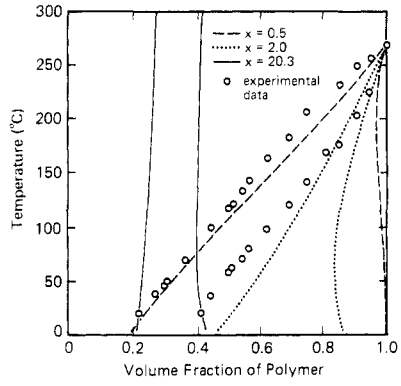

Figure 6. Calculated phase diagrams for $x = 0.5$ (broken lines), $x = 2$ (dotted lines), and $x = 20.3$ (solid lines). The corresponding values of T^* required for matching with experiment at T_{ni} in the first two cases are 4556 and 944 K. In the last case, T^* was set to 124 K, to match the calculated and measured room temperature values of both v_i and v_n. Experimental data have been superimposed on the calculated diagrams as individual symbols.

by choosing a smaller value of x, even though such a choice is inconsistent with the molecular geometry. The condition $x \to 0$ represents an approach to the Maier–Saupe limit,[28] where the shape anisotropy of molecules is ignored and the spontaneous molecular ordering in a nematic phase is modeled in terms of orientation-dependent interactions alone. Figure 6 shows the theoretical predictions for x equal to 2 and 0.5. The boundary between the biphasic field and the single-phase isotropic field does indeed fit the experimental data closely for $x = 0.5$. However, the calculated boundary between the biphasic and single-phase anisotropic fields no longer follows the experimental data even qualitatively in this case. Also, the value of $T^* = 4556$ K required for matching at T_{ni} of the neat polymer is completely unrealistic.

An alternative route to matching the results of theory and experiment is to equate the calculated and measured values of the biphasic concentrations, v_i and v_n, at room temperature. The width of the chimney ($v_n - v_i$) on the theoretical diagram is matched first by changing x, after which the theoretical values can be adjusted on the diagram by changing T^*. Figure 6 shows a best fit obtained when $x = 20.3$ and $T^* = 124$ K. Since this combination emphasizes the hard steric repulsions relative to soft attractions, the predicted phase diagram is a nearly vertical chimney, exhibiting little temperature dependence (and an infinite T_{ni}).

Discussion

It is clear that the observed temperature dependence of biphasic separation does not follow the predictions of the freely jointed rod model.[16] In terms of this model, the axial ratio of the "equivalent rod", or the Kuhn segment, has to change drastically with temperature, from ca. 4 at 260 °C to ca. 20 at 20 °C. Although the flexibility of the spacer groups in the backbone should certainly increase with increasing temperature, such a drastic change is well beyond any reasonable estimate. Such a strong temperature dependence also rules out the wormlike chain models.[8,29] wherein the flexibility increases with temperature but only modestly.

The observed phase diagram therefore demonstrates that a small change in spacer flexibility is magnified enormously in the biphasic separation behavior. This in turn indicates that there exists large "cooperativity" in alignment of neighboring rodlike segments in the ordered state, which is strongly dependent on the "flexibility" of the intervening spacer groups. Qualitatively, this picture is then consistent with the conclusions drawn previously for the nematic melts of semiflexible polymers composed of rodlike and spacer groups in alternating succession, i.e., that polymer chains favor highly extended conformations in the nematic state.[14] In this regard, similar investigations on the chain conformations in nematic solutions will then be very helpful in understanding the phase behavior of semiflexible polymers.

Previously, Krigbaum[30] and Ciferri and Marsano[31] studied the temperature dependence of the biphasic behavior of other semiflexible polymers such as poly(*n*-hexyl isocyanate) and cellulose derivatives. By carrying out separate measurements of persistence lengths in dilute solutions at various temperatures, they found that their phase behavior is in good agreement with the predictions of the freely jointed rod model. One should note, however, that those polymers studied by Krigbaum and by Ciferri et al. contain no spacer groups and are therefore considerably less flexible than our polymer. The lack of well-defined rodlike moieties exhibiting strong orientation-dependent interactions may be responsible for the apparent lack of cooperative alignment in their polymers. Closer comparison of the predicted and experimental phase diagrams of Krigbaum and of Ciferri et al., however, shows that a better agreement requires a longer Kuhn segment length than measured in dilute solutions, indicating some tendency for cooperative alignment in the nematic phase. Hence, it is likely that the degree of cooperative alignment in the nematic phase is dependent on the chain model itself.

Concerning theory, our experimental results also suggest a new model emphasizing cooperative alignment of adjacent rodlike segments that is coupled very closely to the conformational characteristics of the intervening spacer groups. An attempt in this direction was started by Flory and Matheson,[32] who modeled the chains with interconvertible rodlike and random-coil sequences in equilibrium. Though their calculations are aimed at the biphasic equilibria of polymers (polypeptides) undergoing helix–coil transitions and exhibiting no anisotropic interactions, they indeed show that the incipient volume fraction for stability of the nematic solution varies very strongly with the degree of helicity or flexibility. In the case of semiflexible polymers comprising aromatic rodlike moieties connected by flexible spacer groups, theory should be reformulated to take into account the fixed length of each rodlike moiety

and spacer group, as well as the contributions from significant orientation-dependent anisotropic interactions.[33]

Acknowledgment. We thank IBM (U.K.) for awarding a Visiting Scientist Fellowship to C.V.

Registry No. (ClCOC$_6$H$_4$-*p*-O(CH$_2$)$_6$OC$_6$H$_4$-*p*-COCl)(2,4-(HO)$_2$C$_6$H$_3$(CH$_2$)$_6$O-*p*-C$_6$H$_4$N=NC$_6$H$_4$-*p*-OCH$_3$) (copolymer), 121157-62-8; (ClCOC$_6$H$_4$-*p*-O(CH$_2$)$_6$OC$_6$H$_4$-*p*-COCl)(2,4-(HO)$_2$C$_6$H$_3$(CH$_2$)$_6$O-*p*-C$_6$H$_4$N=NC$_6$H$_4$-*p*-OCH$_3$) (SRU), 104167-11-5.

References and Notes

(1) Presented in part at the American Chemical Society Meeting, Toronto, June 1988; *Polym. Prepr. (Am. Chem. Soc., Div. Polym. Chem.)* **1988**, *29*(1), 484.
(2) IBM World Trade Visiting Scientist. Current address: Department of Materials Science and Engineering FB-10, University of Washington, Seattle, WA 98195.
(3) Flory, P. J. *Adv. Polym. Sci.* **1984**, *59*, 1.
(4) Itou, T.; Teramoto, A. *Macromolecules* **1984**, *17*, 1419.
(5) Flory, P. J.; Irvine, P. A. *J. Chem. Soc., Faraday Trans. 1* **1984**, *80*, 1807; **1984**, *80*, 1821.
(6) Ballauff, M.; Flory, P. J. *Ber. Bunsenges. Phys. Chem.* **1984**, *88*, 530.
(7) Flory, P. J. *Macromolecules* **1978**, *11*, 1138.
(8) Ronca, G.; Yoon, D. Y. *J. Chem. Phys.* **1985**, *83*, 373.
(9) Maier, W.; Saupe, A. *Z. Naturforsch.* **1959**, *14a*, 882.
(10) Roviello, A.; Sirigu, A. *J. Polym. Sci. (Lett.)* **1975**, *13*, 455.
(11) *Liquid Crystalline Order in Polymers*; Blumstein, A., Ed.; Academic Press: New York, 1978.
(12) *Polymer Liquid Crystals*; Ciferri, A., Krigbaum, W. R., Meyer, R. B., Eds.; Academic Press: New York, 1982.
(13) Ober, C. K.; Jin, J.-I.; Lenz, R. W. *Adv. Polym. Sci.* **1984**, *59*, 103.
(14) Yoon, D. Y.; Bruckner, S.; Volksen, W.; Scott, J. C.; Griffin, A. C. *Faraday Discuss. Chem. Soc.* **1985**, *79*, 41. Yoon, D. Y.; Bruckner, S. *Macromolecules* **1985**, *18*, 651.
(15) Warner, M.; Flory, P. J. *J. Chem. Phys.* **1980**, *73*, 6327.
(16) Flory, P. J. *Macromolecules* **1978**, *11*, 1141.
(17) Reck, B.; Ringsdorf, H. *Makromol. Chem., Rapid Commun.* **1986**, *7*, 389.
(18) Reck, B. Ph.D. Thesis, Institut für Organische Chemie, Universität Mainz, FRG, 1988.
(19) Viney, C.; Windle, A. H. *Liq. Cryst.* **1986**, *1*, 379.
(20) Papkov, S. P. In *Contemporary Topics in Polymer Science*; Pearce, E. M., Schaefgen, J. R., Eds.; Plenum: New York, 1977; pp 97–108.
(21) McKie, D.; McKie, C. H. *Crystalline Solids*; Nelson: London, 1974; p 512.
(22) Werbowyj, R. S.; Gray, D. G. *Macromolecules* **1980**, *13*, 69.
(23) Aharoni, S. M. *Polym. Prepr. (Am. Chem. Soc., Div. Polym. Chem.)* **1981**, *22*, 116.
(24) Aharoni, S. M. *Mol. Cryst. Liq. Cryst. (Lett.)* **1980**, *56*, 237.
(25) Alderman, N. J.; Mackley, M. R. *Faraday Discuss. Chem. Soc.* **1985**, *79*, 149.
(26) Rojstaczer, S.; Stein, R. S. *Mol. Cryst. Liq. Cryst. Including Nonlinear Opt.* **1988**, *157*, 293.
(27) Greenspan, D. *Discrete Numerical Methods in Physics and Chemistry*; Academic Press: New York, 1974; pp 12–22.
(28) Flory, P. J.; Ronca, G. *Mol. Cryst. Liq. Cryst.* **1979**, *54*, 311.
(29) Khokhlov, A. R., Semenov, A. N. *J. Stat. Phys.* **1985**, *38*, 161.
(30) Krigbaum, W. R. *Faraday Discuss. Chem. Soc.* **1985**, *79*, 133 and the references therein.
(31) Ciferri, A.; Marsano, E. *Gazz. Chim. Ital.* **1987**, *117*, 567.
(32) Flory, P. J.; Matheson, R. R. *J. Phys. Chem.* **1984**, *88*, 6606.
(33) Flory, P. J., in press.

A Model for the Curing Reaction of Epoxy Resins

S. Matsuoka, X. Quan,* H. E. Bair, and D. J. Boyle

AT&T Bell Laboratories, Murray Hill, New Jersey 07974. *Received January 17, 1989; Revised Manuscript Received March 20, 1989*

ABSTRACT: A parametric formula describing the curing reaction of cross-linkable polymers and based on the interdependence of the reaction rate and relaxation time is presented. Changes in the relaxation time due to cross-linking are described by analogy with the physical annealing process in glasses. A computer program developed for this study has been found useful in designing the curing process and in predicting the viscoelastic properties of the resulting cured resins. The processing variables that directly affect product reliability can be accurately estimated by this technique.

Introduction

Polymers that can withstand temperatures in excess of 150 °C are found in a wide range of electronic and aerospace applications. Among them, epoxy resins are one of the oldest and most vigorously developed high-temperature polymers in use today. Millions of pounds are produced annually for use in printed circuits, precision connectors, and VLSI encapsulation packages.

Epoxy resins attain their high-temperature properties by virtue of a densely cross-linked molecular network. As in all high-temperature thermosetting resins, the last stage of the curing reaction slows as molecular motion becomes restricted in the highly cross-linked network of polymer molecules. A model for describing curing reactions must include a thermodynamic parameter for the molecular mobility, which changes as the reaction proceeds. Our model is based on the similarity between the cross-linking process and physical aging of thermoplastic (un-cross-linked) glassy polymers. In both cases, chain mobility decreases with time, leading to increased relaxation times. This model can be used to design the optimal temperature–time program for the curing process and to predict the final viscoelastic and thermomechanical properties of the resin being used.

Relaxation Time and Thermodynamic Variables

Assuming that the curing reaction is analogous to the physical aging process, there are two questions that need to be answered. The first question is what kind of distribution of relaxation times is the most appropriate for the curing process. The second question is how the intensive quantities, i.e. the temperature and pressure, and the extensive quantities, i.e. the volume, entropy, and enthalpy, affect the relaxation time of the curing polymer.

(1) Distribution of Relaxation Times. It is agreed by most workers who have studied the glass transition[1–5] that a single relaxation time cannot adequately describe the thermodynamic recovery or physical aging process. One unequivocal proof for this statement can be found in Kovacs' classic experiment of the "memory effect".[1] While several models for the distribution of relaxation times have been suggested by various authors,[2,5] we use a spectrum obtained from dielectric relaxation of poly(vinyl acetate),[5] which gives a good fit for the thermodynamic recovery

0024-9297/89/2222-4093$01.50/0